Optimizing Gold Nanorod Synthesis for Photoacoustic Retinal Stimulation and Biocompatibility

Michael Coppellotti[1,2], Jerry Yu[2,3], Edward Nelson[2], Chen Yang[*,2]

Natick High School, 15 West St., Natick MA 01760[1], Boston University Photonics Center, 8 St. Mary's St, Boston, MA 02215[2], Mt. Lebanon High School, 155 Cochran Rd, Pittsburgh, PA 15228[3]

Introduction

- **Neuromodulation**: selective electrical or chemical stimulation of neurons without traditional drugs; beneficial for **retinal degenerative diseases** which suffer from limited drug efficacy.[1,2]
- **Photoacoustic-enabled neuromodulation:** a non-genetic, high precision, versatile mechanism
  - *Photoacoustic effect:* (1) ns laser pulse absorbed by material (2) heating and thermal expansion (3) ultrasound propagation → stimulate mechanosensitive ion channels.[1,2]
- **Gold nanorods** (AuNRs) provide potential in their photoacoustic conversion efficiency, strongly tunable LSPR, stability, biocompatibility of Au, and functionalization possibilities.[3]
  - Aspect Ratio of 6 → Peak Absorption ~1030 nm.
    - Limited H_2O absorption, limited residual vision interference, and high penetration depth.
  - 50-100 nm size also allows for anterior ocular penetration.
  - Conventional methods utilizing CTAB as a surfactant are limited in their cell capability due to CTAB's inherent cytotoxicity.
- **Goal:** develop a biocompatible gold nanorod solution to undergo the photoacoustic effect and stimulate retinal activity. We target minimally-invasive delivery modalities for ocular delivery, such as in an eye-drop.

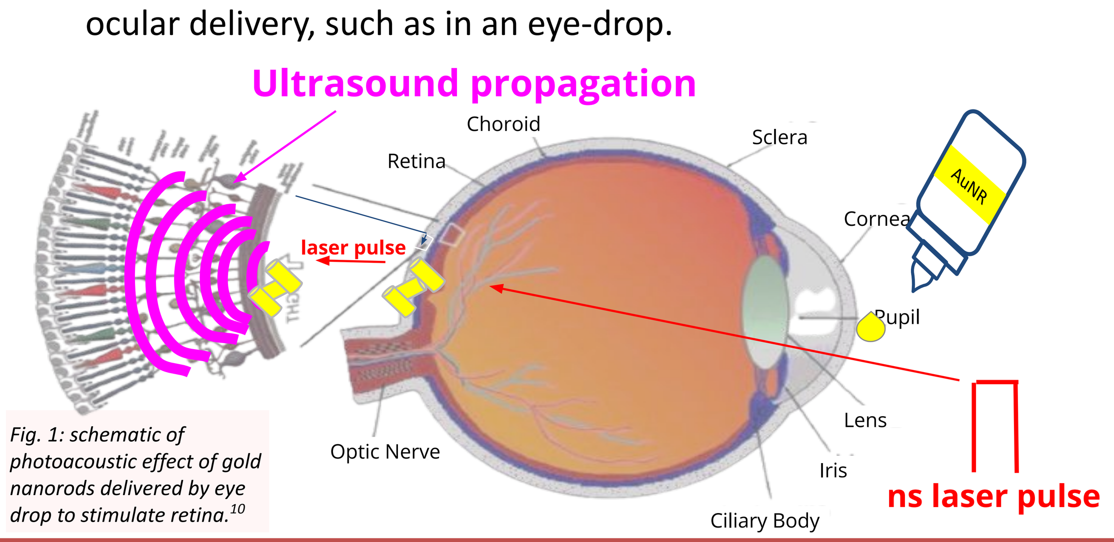

Fig. 1: schematic of photoacoustic effect of gold nanorods delivered by eye drop to stimulate retina.[10]

Methods

To tune the aspect ratio and thus absorption peak, volumes and concentrations of hydrochloric acid (HCl), silver nitrate ($AgNO_3$), seed solution, sodium oleate (NaOL), and cetrimonium bromide (CTAB) can be varied.

- In our synthesis, we report the successful use of a seed-mediated growth[4]
  - Seed Solution: cubic octahedral seeds of Au^0 serving as nucleation sites
    - $HAuCl_4$ (0.25 mL, 0.01 M) introduces Au^{3+} into solution.
    - CTAB (9.75 mL, 0.1 M) dissociates, providing CTA^+ to form micellar complexes with predominantly $AuCl_4^- \rightleftharpoons AuBr_4^-$.
    - $NaBH_4$ (0.6 mL, 0.01 M) rapidly reduces $Au^{3+} \rightarrow Au^0$.
  - Growth Solution: serves to deposit Au^0 on seeds to elongate rods
    - $HAuCl_4$ (25 mL, 0.001 M) introduces Au^{3+} into solution.
    - CTAB (25 mL, 0.0988 M) works as a surfactant and face-specific capping agent.
    - NaOL (0.1234 g into CTAB solution; resultant 0.0162 M) works as a surfactant and initiates the reduction of $Au^{3+} \rightarrow Au^+$.
    - $AgNO_3$ (0.004 M) selectively binds to the {250} facet of the cubic octahedron seed to promote anisotropic growth in the <001> direction[5].
    - HCl (12.1 M) lowers the pH and controls the growth of rods by slowing down $C_6H_8O_6$ reduction.
    - $C_6H_8O_6$ (0.125 mL, 0.064 M) reduces $Au^+ \rightarrow Au^0$.

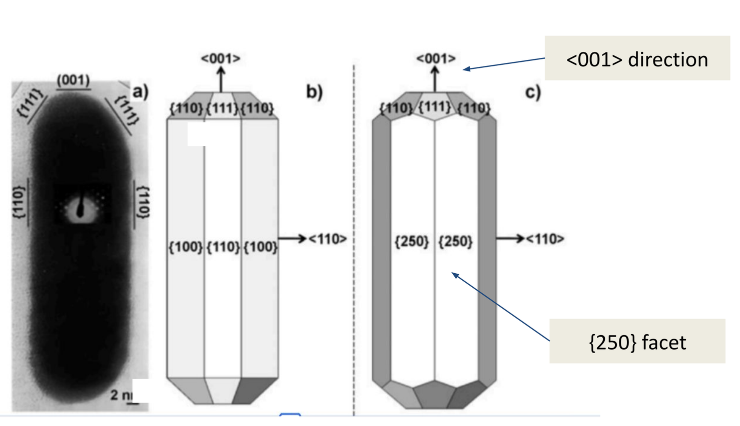

Fig. 2: Schematic of Gold Nanorod facets after elongation from cubic octahedral seed.[5]

- Biocompatibility was tested via an MTT assay on SD rat cortical neurons, assessing the effect of AuNR mass concentration and number of rounds of centrifugation on cell viability.

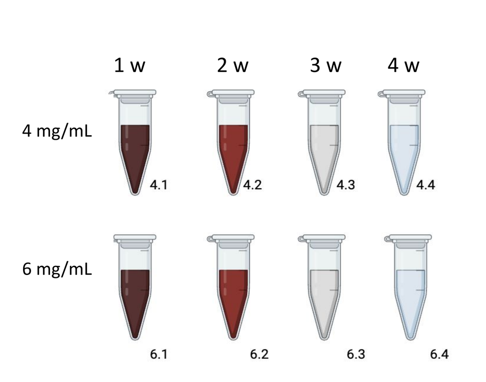

	1	2	3	4	5	6
A	4.1	4.1	4.1	6.1	6.1	6.1
B	4.2	4.2	4.2	6.2	6.2	6.2
C	4.3	4.3	4.3	6.3	6.3	6.3
D	4.4	C	C	C	C	6.4

Fig. 3: schematic of MTT assay set-up for varying treatments of AuNR.

Created in https://BioRender.com

Results

Seed and Growth Solutions:

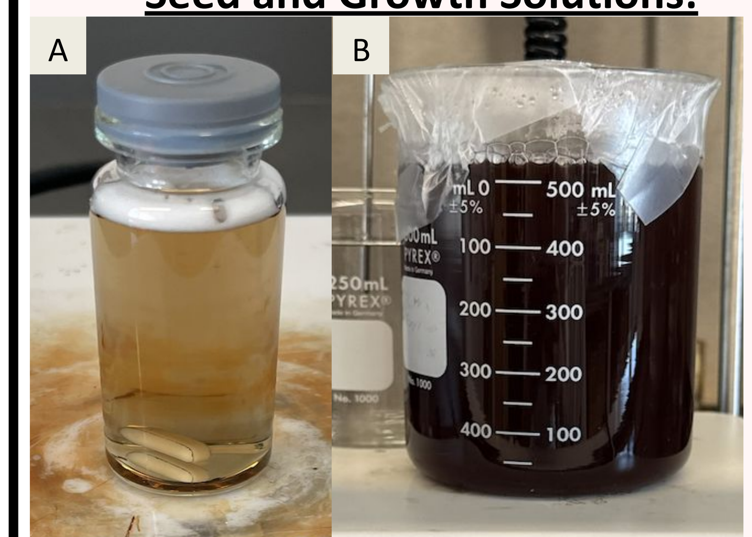

Fig. 4: (A) quality seed solution displaying a yellow-brown color. (B) growth solution ~18 hours after injection of seed, displaying a red-purple hue.

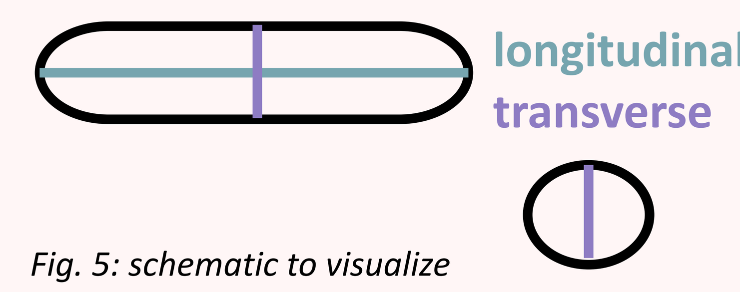

Fig. 5: schematic to visualize the shared transverse mode of LSPR between nanorods and nanospheres; longitudinal LSPR is unique to nanorods

Optimizations of Syntheses:

Fig. 6: UV-Vis Spectrum of AuNR with 0.32 mL HCl and 3.6 mL $AgNO_3$.

UV-Vis AuNR Spectra will exhibit two modes of LSPR absorption: the transverse and longitudinal. Au nanospheres share this transverse mode of absorption, and thus the peaks in the 500 nm range can be indicators of the transverse absorption of rods or of spherical impurities. Additionally, ~1030 nm was successfully targeted by balancing 0.32 mL HCl with 3.6 mL $AgNO_3$.

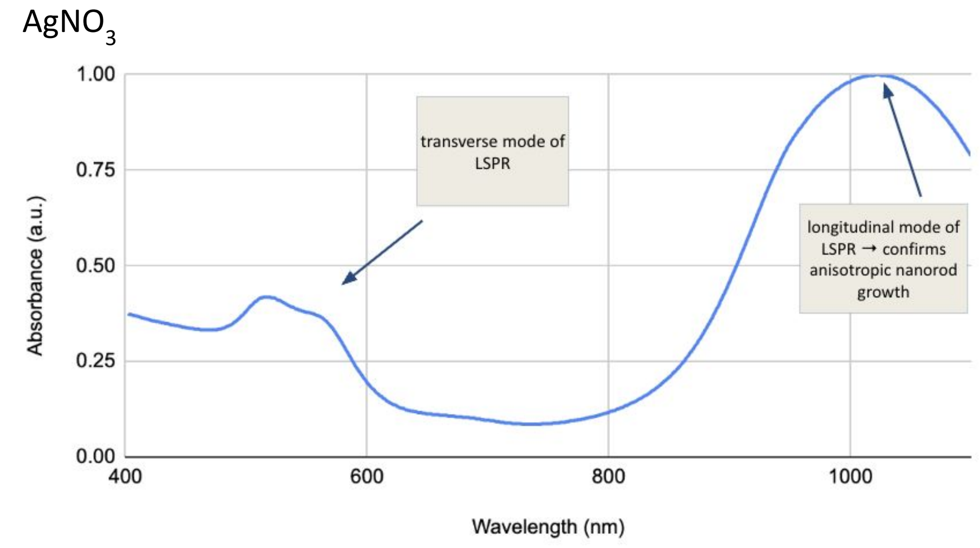

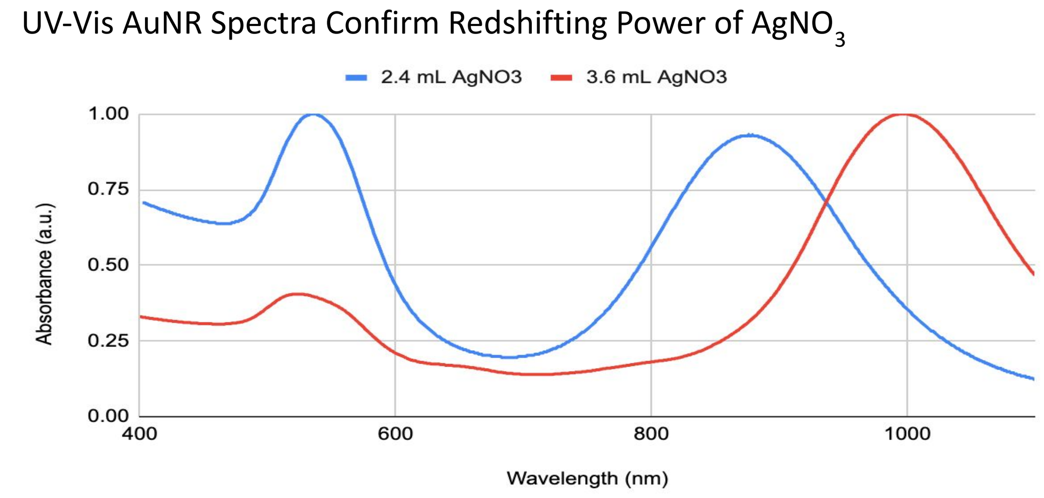

Fig. 7: UV-Vis Spectra demonstrate peak absorption redshift as the amount of $AgNO_3$ increases.

This is due to the selective binding of $AgNO_3$, promoting anisotropic growth. It should be duly noted that the trial with 2.4 mL $AgNO_3$ had glassware cleaned with soap and water, whereas the 3.6 mL trial included ethanol-cleaned glassware.

Fig. 8: UV-Vis Spectra demonstrate peak absorption redshift as the amount of HCl increases.

This is due to an induced kinetic control of the reduction power of ascorbic acid. A more controlled and slower growth allows for anisotropy with adequate time for CTAB and $AgNO_3$ to selectively bind to facets that promote such growth.

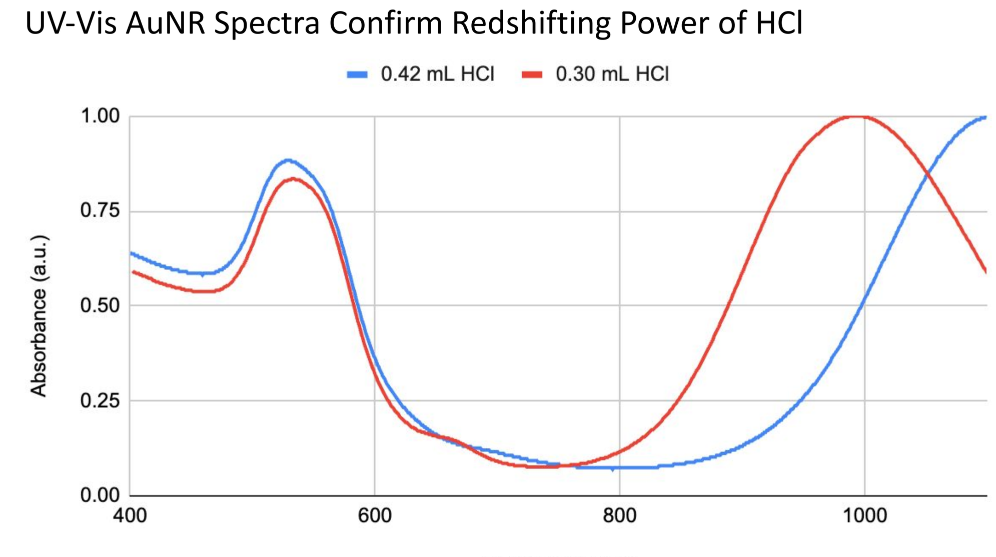

Cytotoxicity Study:

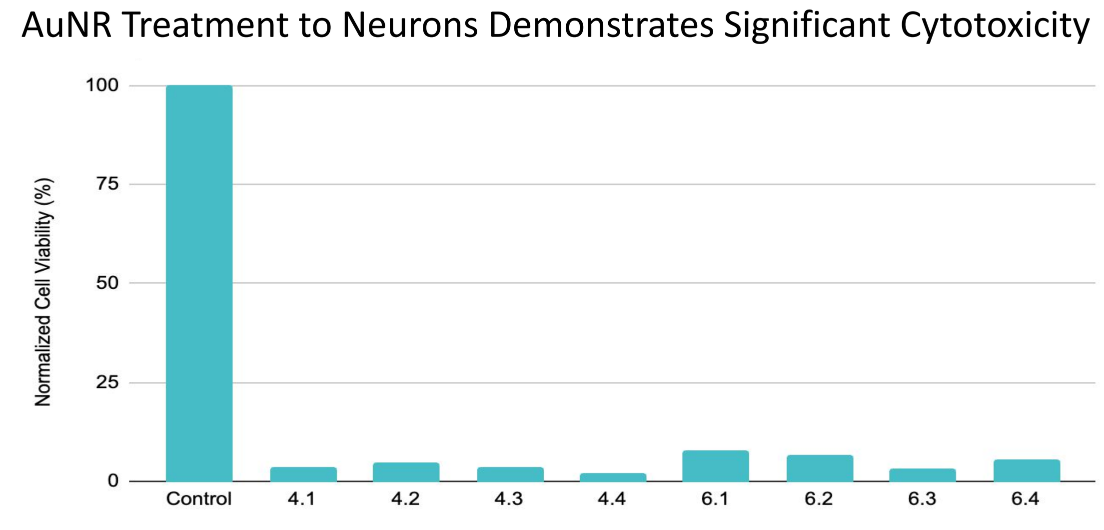

Fig. 9: Relative % Cell Viability, as measured by the MTT assay, for neurons treated with AuNR at 4 mg/mL and 6 mg/mL with varied numbers of washes. The data have been normalized to untreated control neurons. Conditions 4.1-4.3 and 6.1-6.3 represent an average of 3 trials each.

An evident cytotoxicity can be observed by AuNR treatment, with each trial exhibiting significantly less viability than the control.

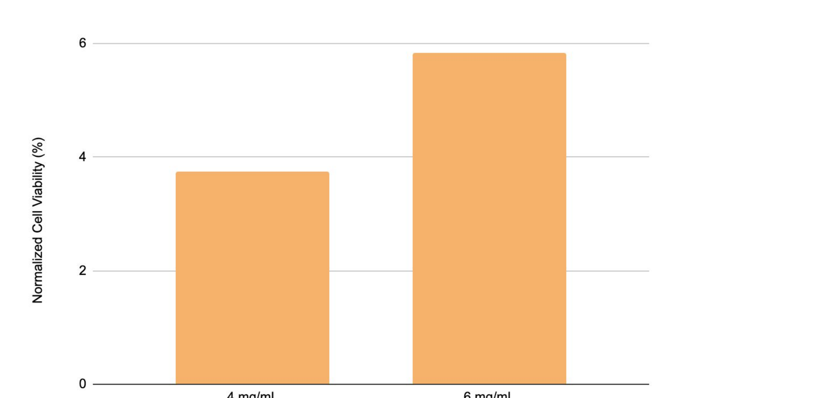

Fig. 10: Relative % Cell Viability averaged between varied numbers of washes (1-4) for respective concentrations of 4 mg/mL and 6 mg/mL.
A clear trend of increased cell viability at higher concentrations is observed.

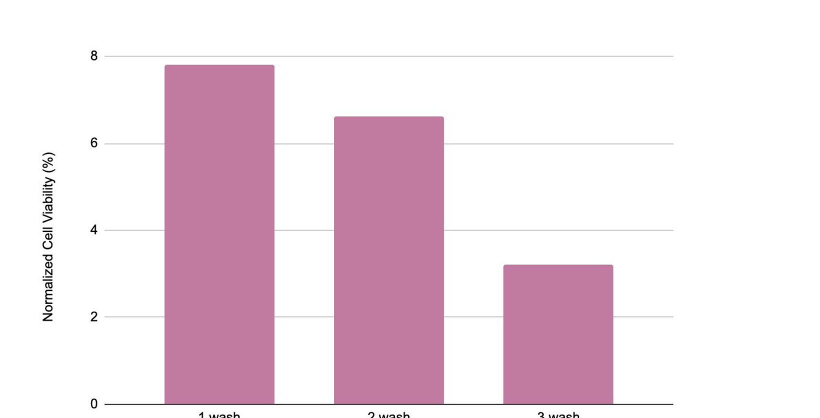

Fig. 11: Relative % Cell Viability averaged, holding the concentration constant at 6 mg/mL, for varied numbers of washing rounds from 1 to 3.
An evident trend of decreased cell viability at increased rounds of centrifugation is observed.

Conclusion

- Successful synthesis of gold nanorods at peak absorption of ~1030 nm with a balance of HCl and $AgNO_3$ volumes (ex. 0.32 mL 12.1 M HCl, 3.6 mL 4 mM $AgNO_3$).
  - Successful slowing of reduction kinetics with additive HCl and anisotropic control with $AgNO_3$.
- Post-synthesis characterization by UV-Vis Spectrophotometry demonstrated a narrow full-width half maximum LSPR peak, indicating homogeneity and monodispersity.
  - Peak of transverse absorption at ~⅓ of longitudinal, indicating low concentration of spherical impurities.
  - Full width at half maximum was ~150-250 nm, illustrating nanorod monodispersity.
- Best practice included cleaning glassware with ethanol, and improved purity was reported with aqua-regia cleaned glassware.
- MTT Assay confirmed the cytotoxicity of AuNR at 4 mg/mL and 6 mg/mL, even with up to 4 washes: highest avg. viability overall ~7.78%.
- Contrary to our initial hypothesis about AuNR concentration on cell viability, the 6 mg/mL application resulted in, on average, higher % cell viability than that of the 4 mg/mL treatment.
- The number of washes did not show a positive correlation with cell viability; in the 6 mg/mL condition, it showed a negative correlation.
  - These unexpected results are likely to be the result of assay interference by AuNR, potentially inflating absorption readings. Alternative explanations could point to dissimilar cellular uptake methods due to aggregated particles.

Next Steps

- Explore CTAB-free synthesis methods, such as C_{12}EDMAB as an alternative surfactant[6]
- Functionalize CTAB-containing nanorods after synthesis by surface modification: PEI silane, MUA, PEG, etc.[7,8,9]
- Apply less AuNR solution for initial incubation when completing MTT Assay to achieve higher absorbance readings
- Suspend AuNR in PBS before application to cells in MTT Assay rather than water
- Conduct another cell viability assay, such as an ATP assay
- Ensure nanorods do not aggregate before performing cytotoxicity assays

References

(1)
Du, Z.; Chen, G.; Li, Y.; Zheng, N.; Cheng, J.-X.; Yang, C. Photoacoustic: A Versatile Nongenetic Method for High-Precision Neuromodulation. *Accounts of Chemical Research* **2024**, *57* (11), 1595–1607. https://doi.org/10.1021/acs.accounts.4c00119.

(2)
Jiang, Y.; Huang, Y.; Luo, X.; Wu, J.; Zong, H.; Shi, L.; Cheng, R.; Zhu, Y.; Jiang, S.; Lan, L.; Jia, X.; Mei, J.; Man, H.-Y.; Cheng, J.-X.; Yang, C. Neural Stimulation in Vitro and in Vivo by Photoacoustic Nanotransducers. *Matter* **2021**, *4* (2), 654–674. https://doi.org/10.1016/j.matt.2020.11.019.

(3)
Park, S.; Nguyen, V. P.; Wang, X.; Paulus, Y. M. Gold Nanoparticles for Retinal Molecular Optical Imaging. *International Journal of Molecular Sciences* **2024**, *25* (17), 9315–9315. https://doi.org/10.3390/ijms25179315.

(4)
Ye, X.; Zheng, C.; Chen, J.; Gao, Y.; Murray, C. B. Using Binary Surfactant Mixtures to Simultaneously Improve the Dimensional Tunability and Monodispersity in the Seeded Growth of Gold Nanorods. *Nano Letters* **2013**, *13* (2), 765–771. https://doi.org/10.1021/nl304478h.

(5)
Carbó-Argibay, E.; Rodríguez-González, B.; Gómez-Graña, S.; Guerrero-Martínez, A.; Pastoriza-Santos, I.; Pérez-Juste, J.; Liz-Marzán, L. M. The Crystalline Structure of Gold Nanorods Revisited: Evidence for Higher-Index Lateral Facets. *Angewandte Chemie International Edition* **2010**, *49* (49), 9397–9400. https://doi.org/10.1002/anie.201004910.

(6)
Allen, J. M.; Xu, J.; Blahove, M.; Canonico-May, S. A.; Santaloci, T. J.; Braselton, M. E.; Stone, J. W. Synthesis of Less Toxic Gold Nanorods by Using Dodecylethyldimethylammonium Bromide as an Alternative Growth-Directing Surfactant. *Journal of Colloid and Interface Science* **2017**, *505*, 1172–1176. https://doi.org/10.1016/j.jcis.2017.06.101.

(7)
Han, H.-W.; Joe, A.; Jang, E.-S. Reduced Cytotoxicity of CTAB-Templated Silica Layer on Gold Nanorod Using Fluorescence Dyes and Its Application in Cancer Theranostics. *Journal of Industrial and Engineering Chemistry* **2021**, *96*, 202–212. https://doi.org/10.1016/j.jiec.2021.01.020.

(8)
Shi, X.; Perry, H. L.; D E T Wilton-Ely, J. Strategies for the Functionalisation of Gold Nanorods to Reduce Toxicity and Aid Clinical Translation. *Nanotheranostics* **2021**, *5* (2), 155–165. https://doi.org/10.7150/ntno.56432.

(9)
He, J.; Unser, S.; Bruzas, I.; Cary, R.; Shi, Z.; Mehra, R.; Aron, K.; Sagle, L. The Facile Removal of CTAB from the Surface of Gold Nanorods. *Colloids and Surfaces B: Biointerfaces* **2017**, *163*, 140–145. https://doi.org/10.1016/j.colsurfb.2017.12.019.

(10)
Kolb, H. *Simple Anatomy of the Retina by Helga Kolb – Webvision*. Utah.edu. https://webvision.med.utah.edu/book/part-i-foundations/simple-anatomy-of-the-retina/.

Acknowledgements

A big thank you to all of the members of the Yang Lab who assisted in this research project and offered invaluable feedback for this poster: Dr. Yueming Li, Zhiyi Du, Guo Chen, and Deming Li. Thank you also to Dr. Chen Yang for admitting me into her lab for the summer and allowing me to explore photoacoustic neuromodulation under the mentorship of Teddie Nelson. Lastly, I would like to thank the RISE program for setting up this mentorship opportunity.